

## Positron Annihilation with Inner-Shell Electrons in Noble Gas Atoms

Koji Iwata,<sup>1</sup> G. F. Gribakin,<sup>2</sup> R. G. Greaves,<sup>1</sup> and C. M. Surko<sup>1</sup>

<sup>1</sup>*Physics Department, University of California, San Diego, La Jolla, California 92093-0319*

<sup>2</sup>*School of Physics, University of New South Wales, Sydney 2052, Australia*

(Received 12 February 1997)

Measurements are presented of the Doppler broadening of the 511-keV  $\gamma$ -ray line from thermalized positrons annihilating with Ar, Kr, and Xe. The experiments are conducted at low pressures using positrons stored in a Penning-Malmberg trap, which ensures that only two-body interactions are involved. The contributions from annihilation on inner-shell electrons are studied quantitatively in an isolated atomic system for the first time. The spectra are compared with theoretical calculations using a simple Hartree-Fock model to identify the inner-shell contributions. [S0031-9007(97)03508-4]

PACS numbers: 34.50.-s, 36.10.-k, 71.60.+z, 78.70.Bj

Positron-matter interactions have been studied extensively and are a field of active research [1–8]. A unique aspect of these interactions is the emission of two 511-keV  $\gamma$  rays when a positron annihilates with an electron. This signal provides information about the interaction, and it is the basis of many types of measurements. For example, this signal has been used to characterize defects [2] and interfaces [3] in solids. One type of measurement is the observation of the emitted  $\gamma$ -ray directions and energies, which provide the momenta of annihilating pairs. In the case of bound electrons, the momentum distribution is dominated by that of the electron wave function [4,5]. The  $\gamma$ -ray directions can be measured by the angular correlation of annihilation radiation technique [6], while the energies can be measured directly using high-resolution  $\gamma$ -ray spectroscopy [1].

Positrons annihilate predominantly with valence electrons in insulators or with conduction electrons in metals because of the repulsive potential exerted on the positron by the nuclei. However, a small fraction of the positrons can tunnel through this repulsive potential and annihilate with inner-shell electrons. In the work presented here, we detect inner-shell annihilation by measuring the momentum distribution of the annihilating electron-positron pairs by the Doppler broadening of the annihilation  $\gamma$  rays. Inner-shell annihilation has been studied previously for positrons interacting with condensed matter targets using a clever coincidence technique with two detectors [7,8]. This technique improves the signal-to-noise ratio, which in turn enables one to explore the high momentum region of the spectra. However, we have been able to obtain sufficiently good statistics to identify inner-shell annihilation using a single detector.

The interactions in condensed matter are very different from the isolated interaction of a positron with a single atom discussed here. For example, in metals the positron forms a Bloch wave under the periodic potential generated by the ions, while positron annihilation in a single atom is a scattering process. We have developed a method for studying interactions between positrons and isolated atoms and molecules using cold positrons stored in a modified

Penning trap [9]. The positrons can be confined for a long time [10] so that they can be used efficiently. Their energies are below the positronium formation thresholds of the substances under study so that the annihilation signal from positronium is absent. Since the introduction of positron trapping techniques, a wide range of experiments have been carried out. They include measurements of annihilation rates for a variety of molecules [11] and the temperature dependence of annihilation rates for the noble gases [12], simulations of astrophysical positron annihilation [4], and measurement of the Doppler broadening of the annihilation line for various substances [4,5,13].

In this Letter we present precise measurements of the annihilation  $\gamma$ -ray spectra for Ar, Kr, and Xe. The measured spectra are compared with calculations based on the Hartree-Fock (HF) approximation. The high momentum components in the spectra provide a quantitative measure of the fraction of positrons that annihilate with inner-shell electrons. This is the first experimental study of positrons annihilating with inner-shell electrons in isolated two-body positron-atom interactions.

The measurements are performed in a modified Penning-Malmberg trap designed to accumulate large numbers of positrons [9,14]. The positrons are confined electrostatically in the axial direction and magnetically ( $B = 1000$  G) in the radial direction (see Fig. 1). High energy positrons emitted from a 40-mCi  $^{22}\text{Na}$  radioactive source are moderated to a few eV. Through inelastic collisions with a  $\text{N}_2$  buffer gas, the positrons are trapped in a potential well provided by the electrodes. The positrons reach thermal equilibrium with  $\text{N}_2$  on the order of 1 s, resulting in a positron temperature of  $\sim 300$  K [14].

Measurements of the  $\gamma$ -ray spectra are performed using a technique similar to previous measurements [4,13]. Data are recorded in repetitive cycles of positron filling and annihilation. Positrons are accumulated in the last stage of the Penning trap (see Fig. 1) for a fixed amount of time (typically 5 s) in the presence of a  $\text{N}_2$  buffer gas at a pressure of  $5 \times 10^{-7}$  torr. After a 1-s positron cooling time, the buffer gas is shut off and pumped out for 8 s to ensure that annihilation on  $\text{N}_2$  (lifetime on  $\text{N}_2 > 300$  s)

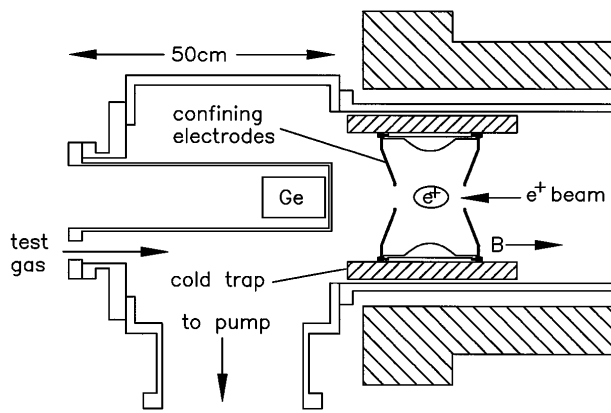


FIG. 1. Last stage of the positron trap showing the annihilation region and the Ge  $\gamma$ -ray detector.

does not contribute significantly to the measured  $\gamma$ -ray spectra. A multichannel analyzer (MCA) is then gated on to record annihilation  $\gamma$  rays measured by a high resolution Ge detector, and the test gas (lifetime on test gas  $\sim 5$  s) is introduced to begin the annihilation phase of the cycle. After the measurement period, typically 5 s, the test gas feed and MCA are switched off. These cycles were repeated for 12 h for Ar and Kr and for 58 h for Xe. The spectra were taken in 1-h time segments, and the drift in the detector (less than 0.01 keV in 12 h) was carefully monitored. The number of positrons in each fill was adjusted to minimize  $\gamma$ -ray pileup.

The measured spectra contain the annihilation peak, a constant background, and a step function convolved with the line shape of the main peak. The main peak represents the intrinsic line shape convolved with the detector response, which can be approximated with a Gaussian. The step function is due to Compton scattering in the detector crystal. In order to model the effects of the step function and the baseline, the main peak was first fitted with a Gaussian. The step function and the baseline were then subtracted, after convolution of the step function with the fitted Gaussian width. The amplitudes of the step function and the baseline were determined by requiring that the spectrum be zero at energies far (e.g., 15 keV) from the centroid of the peak (511 keV).

The corrected spectra for Xe, Kr, and Ar are shown in Figs. 2, 3, and 4, respectively. The error bars represent the expected statistical variation in spectral amplitude due to counting statistics. The high quality of these data relative to previous measurements in isolated two-body systems [13] is a consequence of improvements to the positron moderator, experimental geometry, and gas handling systems [4]. The spectra can be resolved over 4 orders of magnitude in spectral amplitude, and this is crucial in separating the contribution to the annihilation signal due to inner-shell electrons from that due to electrons in the outer-most shell. In Figs. 2, 3, and 4, only the high energy side of the symmetric  $\gamma$ -ray line is shown, since this region

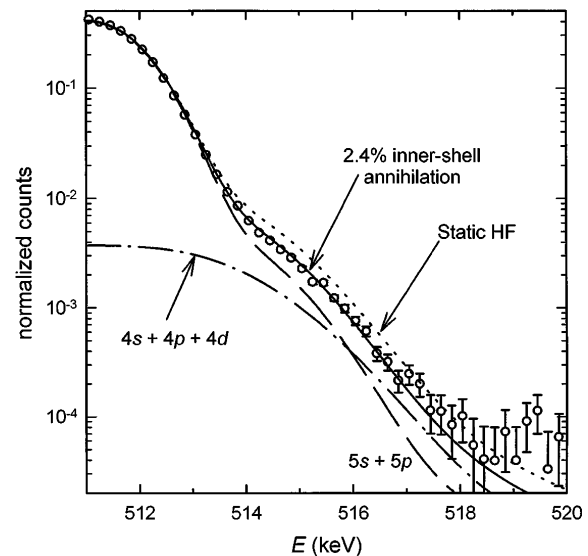


FIG. 2. The Doppler-broadened  $\gamma$ -ray spectrum resulting from positrons annihilating on Xe atoms at  $p = 2 \times 10^{-6}$  torr. Shown are the experimental data ( $\circ$ ), the static Hartree-Fock calculation ( $\cdots$ ), the best fit to the data ( $-$ ), which includes a 2.4% contribution from the states with principle quantum number  $(n - 1) = 4$ , the contribution from the outer-shell states with  $n = 5$  ( $- - -$ ), and that from the inner-shell states with  $(n - 1) = 4$  ( $- \cdot -$ ).

has greater statistical significance due to absence of the Compton scattering component. The measured and calculated spectra are normalized so that  $\int_0^\infty f(E) dE = 1$ , where  $f(E)$  is the amplitude of the spectrum at  $\gamma$ -ray energy,  $E$ . The theoretically predicted spectra shown in Figs. 2, 3, and 4 have been convolved with the Gaussian detector response, which has a full width at half maximum (FWHM) of 1.16 keV.

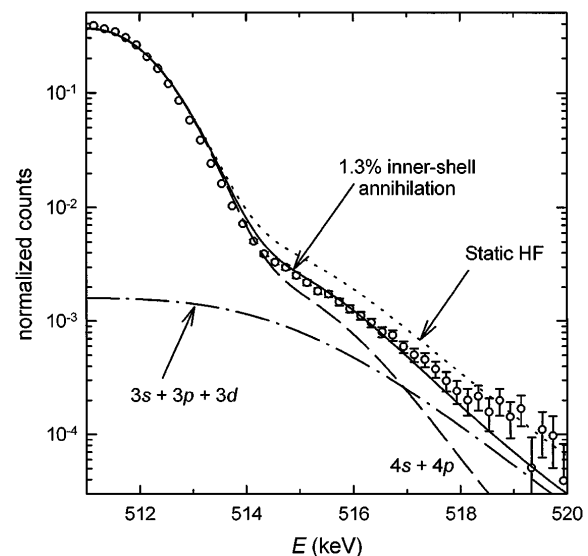


FIG. 3. The Doppler-broadened  $\gamma$ -ray spectrum resulting from positrons annihilating on Kr atoms at  $p = 9 \times 10^{-6}$  torr. The notation is similar to that in Fig. 2.

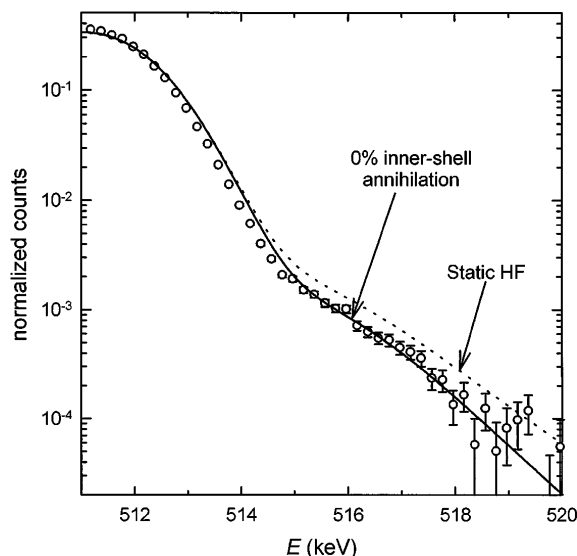


FIG. 4. The Doppler-broadened  $\gamma$ -ray spectrum resulting from positrons annihilating on Ar atoms at  $p = 2 \times 10^{-5}$  torr. The notation is similar to that in Fig. 2.

In order to identify the contributions of inner-shell electrons to the annihilation  $\gamma$ -ray spectra, we calculated the line shapes using the static HF approximation. In this approximation, the wave function of the positron at thermal energies is calculated from the Schrödinger equation using the potential of the HF atomic ground state, and annihilation  $\gamma$ -ray spectra are determined for electrons in each atomic subshell. The annihilation fractions,  $\zeta$ , and the associated line shapes (FWHM),  $\Delta E$ , for electrons from the two outer shells with principal quantum numbers  $n$  and  $n - 1$  are summarized in Table I for Ar, Kr, and Xe ( $n = 3, 4$ , and  $5$ , respectively). The sum of the annihilation fractions for the two outer subshells  $\zeta_{nl}$  and those from the three (or two, for Ar) inner subshells  $\zeta_{(n-1)l}$  is normalized to unity. There is good agreement between the widths and shapes of the  $\gamma$ -ray spectra obtained in the static HF approximation and the experimental data (see Table I and Figs. 2, 3, and 4).

As expected, the main contribution to the annihilation probability comes from the outer-shell electrons. The linewidths from inner-shell annihilation (3.3–9.4 keV) are much larger than those from outer shells (1.4–2.9 keV) due to the higher momenta of the former. The values of  $\zeta_{(n-1)l}$  are roughly proportional to the number of electrons in the  $s$ ,  $p$ , and  $d$  subshells, namely, 2, 6, and 10, respectively. The lack of an inner  $d$  subshell for Ar (only 8 electrons in the inner shell as compared to 18 for Kr and Xe) results in a lower total annihilation fraction from inner-shell electrons relative to Kr and Xe (Table I). The reason for  $\zeta_{(n-1)d}$  in Xe being greater than  $\zeta_{(n-1)d}$  in Kr is the more diffuse character of the  $d$  orbital in Xe; the radial density of the  $(n - 1)d$  orbital in Xe peaks at 0.75 a.u., as compared to 0.4 a.u. for  $(n - 1)d$  in Kr, and the value of  $\Delta E$  is smaller for the  $d$  orbital in Xe.

As can be seen from Figs. 2 and 3, a contribution from the shell with principal quantum number  $(n - 1)$  is essential to account for the shape of the high-energy tail in the spectra of Xe and Kr. However, it appears that the static HF approximation overestimates the values of  $\zeta_{n-1}$  by about a factor of 2. There are positron-electron correlation effects, not treated by the static approximation, which preferentially enhance the annihilation rate for the most weakly bound electrons, i.e., the outer-shell electrons. On the other hand, they do not affect much of the shape of the  $\gamma$ -ray spectra, as suggested by the agreement observed in Figs. 2, 3, and 4. This enables us to treat the fraction of annihilations with the inner-shell electrons as a fitted parameter,  $\zeta_{n-1}^*$ , to obtain a more precise estimate of this effect. Thus, we are able to achieve good agreement (shown as the solid line in Fig. 2) over 4 orders of magnitude in spectral amplitude with  $\zeta_{n-1}^* = 0.024$ , compared with the static HF value of  $\zeta_{n-1} = 0.048$  for Xe (Table I). Figure 3 shows the results of this analysis for Kr, with similarly good agreement for the spectral line shape. In this case, the fitted value  $\zeta_{n-1}^* = 0.013$ , which is approximately 40% of that predicted by the static HF calculation. For Ar (Fig. 4) the comparison between the measurement and the theory cannot accurately determine the contribution of inner-shell

TABLE I. The FWHM of annihilation  $\gamma$ -ray spectra,  $\Delta E$  (in keV), and partial contributions to the annihilation probability from the subshells of noble-gas atoms,  $\zeta$ , calculated in the static Hartree-Fock approximation.

Shell	Ar		Kr		Xe	
	$\Delta E$	$\zeta$	$\Delta E$	$\zeta$	$\Delta E$	$\zeta$
$np$	2.89	0.808	2.56	0.804	2.22	0.791
$ns$	1.86	0.181	1.66	0.164	1.41	0.161
$(n - 1)d$	...	...	8.85	0.021	6.73	0.036
$(n - 1)p$	9.41	0.008	7.65	0.009	5.80	0.009
$(n - 1)s$	5.18	0.003	4.35	0.003	3.34	0.003
Total	2.65	1	2.38	1	2.06	1
Experiment	2.30	...	2.09	...	1.92	...
$(n - 1)$ tot., th.	...	0.012	...	0.033	...	0.048
$(n - 1)$ fit	...	<0.002	...	0.013	...	0.024

annihilation events. We estimate  $\zeta_{n-1}^* < 0.002$ , which is less than 20% of the value predicted by the static theory.

We note that, in the analysis presented in Ref. [8], the high-momenta “shoulder” of the  $\gamma$ -ray spectrum was fitted by the inner-shell annihilation contribution alone. It is clear from our work that the outer-shell annihilation spectra also possess this shoulderlike feature due to oscillations in the structure of the outer-shell electron wave functions. Neglect of this would result in an overestimate of the fraction of inner-shell annihilation.

While we are able to achieve good agreement for the annihilation  $\gamma$ -ray spectra using simple static HF theory, there is considerable evidence that the positron wave function obtained in this approximation is not correct. For example, the HF approximation fails to reproduce positron-atom scattering and seriously underestimates the total annihilation rate [15]. There is a strong attractive potential between the positron and the atom due to polarization of the atom by the electric field of the positron and virtual positronium formation [15,16]. As a result, the actual positron wave function near the atom is much larger than that predicted by the static approximation. There are also short-range correlation effects due to the electron-positron interaction. They enhance the total wave function at small electron-positron separations and further increase the annihilation rate. However, as seen from Figs. 2, 3, and 4, these effects seem to have little influence on the shapes of the  $\gamma$ -ray spectra. In particular, the  $\gamma$ -ray spectra are expected to be insensitive to short-range electron-positron correlation effects, since the spectra depend only on the momentum of the electron-positron pairs, and their center of mass momenta are weakly affected by this correlation. This means that the annihilation spectra are basically determined by the momentum distribution of the atomic electrons, which are described well by the HF approximation.

There are correlational corrections, which can account for the discrepancy between the theoretical and experimental  $\Delta E$  (Table I). As discussed above, correlations also lead to a large enhancement of the annihilation rates, which is greater for the weakly bound outer-shell electrons. Accordingly, the fitted  $\zeta_{(n-1)}^*$  values are smaller than  $\zeta_{(n-1)}$  from the static HF calculation. The fact that accurate calculations of annihilation spectra are feasible, at least for simple atoms, has recently been demonstrated for atomic He [5], where an excellent agreement is achieved between theoretical and experimental results over 3 orders of magnitude in spectral amplitude.

The robust nature of the shapes of the  $\gamma$ -ray spectra in atoms should be of help in analyzing the details of positron interactions in more complicated systems such as molecules and solids. For example, the annihilation  $\gamma$ -ray spectra can provide quantitative information about preferential sites of positron annihilation in molecules [4].

An important implication of the inner-shell annihilation is the emission of Auger electrons and consequent forma-

tion of doubly ionized atoms. The positron-induced Auger electron emission has been observed in condensed matter [17]. The work described here opens up a possibility of the Auger spectroscopy in gaseous media. Our work suggests that the doubly ionized atoms, associated with Auger electron emission, should be observable, e.g., using time-of-flight mass spectrometry [18,19]. We expect high production of doubly ionized atoms for heavier atoms such as Kr and Xe since they have large inner-shell annihilation fractions.

In summary, our experimental results demonstrate that positron annihilation with inner-shell electrons can be studied in a quantitative manner in isolated atomic systems. While a simple static HF calculation was used successfully to identify the inner-shell electron contribution, the relative fraction of annihilations with inner shell electrons is not predicted accurately by this theory. We hope that these results will motivate further theoretical work in this area.

The work at the University of California, San Diego is supported by the National Science Foundation, Grant No. PHY-9600407, and that of G.F.G. by the Australian Research Council. We thank J.W. Darewych, R.J. Drachman, J.W. Humberston, and C. Kurz for useful discussions and E.A. Jerzewski for expert technical assistance.

- 
- [1] P.J. Schultz and K.G. Lynn, *Rev. Mod. Phys.* **60**, 701 (1988); M.J. Puska and R.M. Nieminen, *Rev. Mod. Phys.* **66**, 841 (1994); A.P. Mills, Jr., *Science* **218**, 335 (1982).
  - [2] Z. Tang *et al.*, *Phys. Rev. Lett.* **78**, 2236 (1997).
  - [3] J.P. Peng *et al.*, *Phys. Rev. Lett.* **76**, 2157 (1996).
  - [4] K. Iwata, R.G. Greaves, and C.M. Surko, *Phys. Rev. A* **55**, 3586 (1997).
  - [5] P. Van Reeth *et al.*, *J. Phys. B* **29**, L465 (1996).
  - [6] P.G. Coleman *et al.*, *J. Phys. B* **27**, 981 (1994).
  - [7] K.G. Lynn *et al.*, *Phys. Rev. Lett.* **38**, 241 (1977).
  - [8] P. Asoka-Kumar *et al.*, *Phys. Rev. Lett.* **77**, 2097 (1996).
  - [9] C.M. Surko, M. Leventhal, and A. Passner, *Phys. Rev. Lett.* **62**, 901 (1989).
  - [10] The positron lifetime with the buffer gas in the system and the cold trap chilled to  $-15^\circ\text{C}$  is  $\sim 30$  s. This can be extended to  $\sim 1$  h at a base pressure of  $5 \times 10^{-10}$  torr by filling the cold trap with liquid nitrogen.
  - [11] K. Iwata *et al.*, *Phys. Rev. A* **51**, 473 (1995).
  - [12] C. Kurz, R.G. Greaves, and C.M. Surko, *Phys. Rev. Lett.* **77**, 2929 (1996).
  - [13] S. Tang *et al.*, *Phys. Rev. Lett.* **68**, 3793 (1992).
  - [14] R.G. Greaves, M.D. Tinkle, and C.M. Surko, *Phys. Plasmas* **1**, 1439 (1994).
  - [15] V.A. Dzuba *et al.*, *J. Phys. B* **29**, 3151 (1996).
  - [16] G.F. Gribakin and W.A. King, *J. Phys. B* **27**, 2639 (1994).
  - [17] A. Weiss *et al.*, *Phys. Rev. Lett.* **61**, 2245 (1988).
  - [18] A. Passner *et al.*, *Phys. Rev. A* **39**, 3706 (1989).
  - [19] L.D. Hulett *et al.*, *Chem. Phys. Lett.* **216**, 236 (1993).